FULL PAPER

Dalton
www.rsc.org/dalton

Chelate ring sequence effects on thermodynamic, kinetic and electron-transfer properties of copper(II/I) systems involving macrocyclic ligands with S_4 and NS_3 donor sets †

Semira Galijasevic,[a] Ksenia Krylova,[a] Michael J. Koenigbauer,[a] Gregory S. Jaeger,[b] Jeffery D. Bushendorf,[b] Mary Jane Heeg,[a] Leo A. Ochrymowycz,[b] Michael J. Taschner[c] and David B. Rorabacher*[a]

[a] *Department of Chemistry, Wayne State University, Detroit, MI 48202, USA*
[b] *Department of Chemistry, University of Wisconsin at Eau Claire, Eau Claire, WI 54701, USA*
[c] *Department of Chemistry, University of Akron, Akron, OH 44325, USA*

Received 15th January 2003, Accepted 26th February 2003
First published as an Advance Article on the web 11th March 2003

The kinetic behavior of electron-transfer reactions involving several copper(II/I) complexes has previously been attributed to a dual-pathway "square scheme" mechanism in which changes in the coordination geometry occur sequentially, rather than concertedly, with the electron-transfer step. In the case of 14-membered macrocyclic quadridentate ligand complexes studied to date, the major geometric change appears to be the inversion of two coordinated donor atoms during the overall electron-transfer process. However, the relative importance of these two inversions has been a matter of speculation. In the current investigation, a comparison is made of Cu(II/I) systems involving two pairs of ligands with S_4 and NS_3 donor sets: 1,4,8,11-tetrathiacyclotetradecane ([14]aneS_4-*a*); 1,4,7,11-tetrathiacyclotetradecane ([14]aneS_4-*b*); 1,4,8-trithia-11-azacyclotetradecane ([14]aneNS_3-*a*); and 1,7,11-trithia-4-azacyclotetradecane ([14]aneNS_3-*b*). In each pair of ligands, isomer *a* has the common chelate ring size sequence 5,6,5,6 while isomer *b* has the sequence 5,5,6,6. A crystal structure for $[Cu^{II}([14]aneNS_3\text{-}b)(H_2O)](ClO_4)_2$ demonstrates that, when coordinated to Cu(II), the *b* isomers stabilize the relatively rare ligand conformation designated as conformer II in which one donor atom is oriented opposite to the other three relative to the plane of the macrocycle. This eliminates one of the donor atom inversion steps which normally occurs during Cu(II/I) electron transfer. The copper complexes formed with these *a* and *b* isomers are examined in terms of (i) their $Cu^{II}L$ and $Cu^{I}L$ stability constants, (ii) their $Cu^{II}L$ formation and dissociation rate constants, (iii) their $Cu^{II/I}L$ redox potentials and (iv) their apparent electron self-exchange rate constants. Of the two donor atom inversions which occur in the case of the *a*-isomer complexes, the specific donor atom inversion which is common to the *b*-isomer complexes is judged to exhibit the larger energy barrier. Thus, it is presumed to represent the rate-limiting process responsible for the onset of "gated" electron transfer in previous studies on *a*-isomer complexes.

Introduction

The markedly different coordination geometries preferred by copper(II) (tetragonal or square pyramidal) and copper(I) (tetrahedral) imply that the reduction or oxidation of copper complexes must be accompanied by significant structural changes. Extensive electron-transfer kinetic studies on Cu(II/I) systems involving macrocyclic tetrathiaethers (L)[1–7] and substituted polypyridyls[8–12] have provided evidence that at least part of this structural change occurs as a discrete step either preceding or succeeding the electron-transfer step. The result is a dual-pathway (square scheme) mechanism, illustrated in Fig. 1, in which **O** and **R** are the stable oxidized and reduced complexes, respectively, and **P** and **Q** represent metastable intermediates. The intermediate species **P** and **Q** are presumed to have coordination geometries approximating the geometries of **O** and **R**, respectively, that is, they are distorted relative to the stable geometries normally found for $Cu^{I}L$ and $Cu^{II}L$, respectively. However, the actual geometries of these intermediate species have remained a matter of speculation.

In previous studies on Cu(II/I) macrocyclic tetrathiaether systems, we have suggested that the **O** ⇌ **Q** and **P** ⇌ **R** transformations may represent changes in the conformation of the coordinated macrocycle involving donor atom inversion.[13] Bosnich, Poon and Tobe first noted that 14-membered macrocycles, with alternating ethylene and trimethylene bridges, could

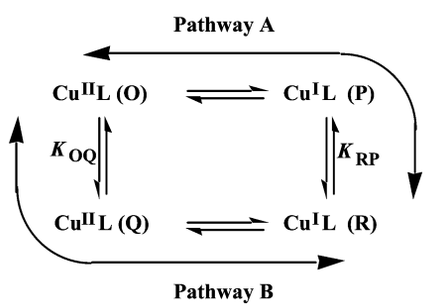

Fig. 1 Dual-pathway square scheme for electron-transfer reactions involving Cu(II/I) macrocyclic complexes. The species labeled **O** and **R** are the stable forms of the Cu(II) and Cu(I) complexes, respectively, while **P** and **Q** represent metastable intermediate species which are presumed to involve geometries resembling the stable form of the opposite oxidation state. The horizontal reactions represent electron transfer and the vertical reactions represent conformational changes.

form metal ion complexes having five distinct ligand conformations if the donor atoms are tetrahedral when coordinated.[14] As illustrated in Fig. 2 for both Cu(II) and Cu(I) macrocyclic ligand complexes, these five conformers are distinguished by the orientations of the coordinated donor atoms. Based on large numbers of crystal structures,[2,4,6,15–22] the predominant ligand conformations for Cu(II) complexes are those designated as conformer I (+ + + +) or conformer III (+ − − +), where the "+" and "−" designations refer to the sequential orientations of either the hydrogen atoms (on nitrogen donors) or the lone pair electrons (on sulfur or oxygen donors) relative to the "plane" of the macrocyclic ring. Crystal structures

† Electronic supplementary information (ESI) available: Tables S1–14: tabulations of experimental rate constants. See http://www.rsc.org/suppdata/dt/b3/b300602f/

DOI: 10.1039/b300602f

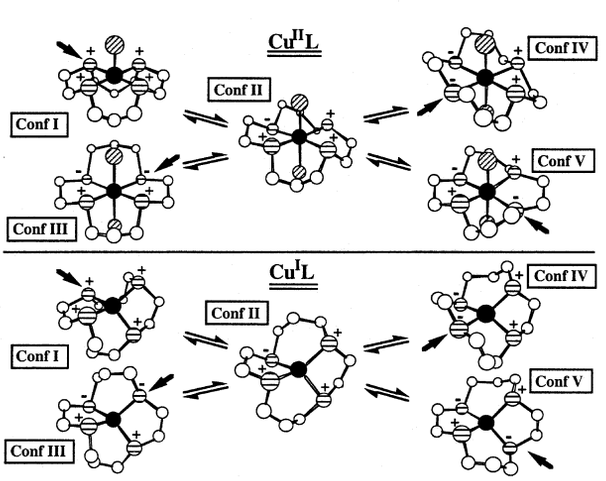

Fig. 2 Conformations formed by Cu(II) and Cu(I) with a coordinated macrocyclic quadridentate ligand forming a 5,6,5,6 chelate ring sequence. The metal ion is represented by a solid circle, the macrocyclic donor atoms by horizontal striping, solvent molecules by diagonal striping, and the carbon atoms by open circles. Hydrogen atoms are omitted for clarity. The "+" or "−" label by each donor atom indicates whether the lone electron pair (in the case of a thiaether sulfur) or attached hydrogen (in the case of an amine nitrogen) is directed above or below the ligand plane. For each conformer, the heavy arrow designates the donor atom which must invert to produce conformer II. (Conformer IV, which has rarely been observed, is considered to represent a "dead end" in the electron-transfer reactions.)

for the corresponding Cu(I) complexes adopt conformer V (+ − + −).[4,6,23] This implies that two donor atoms must invert during the oxidation or reduction of copper. We have postulated that the two donor atom inversions occur sequentially rather than concertedly so that, during the course of an electron-transfer reaction, the ligand must pass through conformer II in which one donor atom is oriented in a direction opposite to the other three (+ − + +).[13]

The electron-transfer step itself is presumed to occur without a significant change in ligand conformation, that is, the precursor and successor $Cu^{II}L$ and $Cu^{I}L$ species in any electron-transfer step represent the same conformer. The conversion of $Cu^{II}L$(O) to $Cu^{I}L$(R) must then entail two intermediate species to generate a theoretical stepladder mechanism (Fig. 3)[13] in which three pathways are possible: (i) **O** ⇌ **Y** ⇌ **Z** ⇌ **R**, (ii) **O** ⇌ **W** ⇌ **Z** ⇌ **R**, and (iii) **O** ⇌ **W** ⇌ **X** ⇌ **R**. In electron-transfer studies conducted to date on Cu(II/I)-macrocyclic tetrathiaether complexes, evidence for only one intermediate has been observed for either pathway A or B (Fig. 1).[1–7] Thus, it has not been possible to determine which conformational changes are involved in the onset of "gating" (*i.e.*, rate-limiting conformational change), as observed in the oxidation of several $Cu^{I}L$ complexes. In other words, it is unknown whether intermediate **P** represents conformer III (or I) or conformer II (*i.e.*, species **Y** or **Z** in Fig. 3) and, as a corollary, whether intermediate **Q** represents conformer II or conformer V (*i.e.*, species **W** or **X** in Fig. 3).[13]

The foregoing considerations led us to speculate that, if a Cu(II) complex could be generated in which the macrocyclic ligand preferentially adopted conformer II (rather than conformer I or III), species **O** and **Y** would be eliminated from consideration, thereby making it possible to assess the impact of the single remaining donor atom inversion which would occur during electron transfer, namely, conformer II ⇌ conformer V. Conformer II is extremely rare in metal complexes having a 5,6,5,6 chelate ring sequence. In a recent examination of all 139 structures in the Cambridge Structural Database involving complexes of Ni(II) with 1,4,8,11-tetraazacyclotetradecane (cyclam or [14]aneN$_4$-*a*) (Fig. 4) and its substituted derivatives, Donnelly and Zimmer found no examples in which

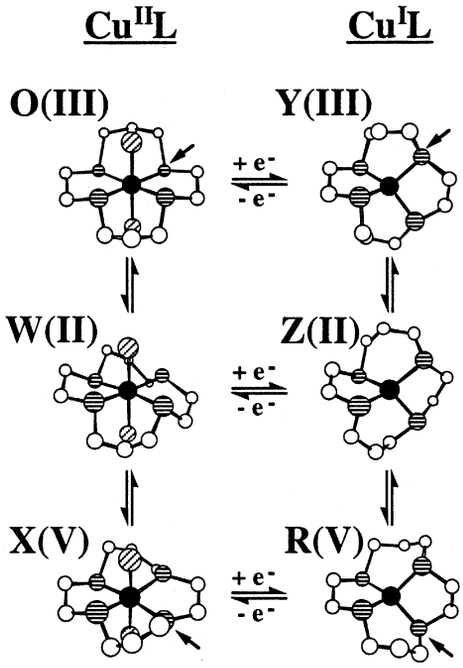

Fig. 3 Proposed stepladder mechanism for the reduction of a Cu(II) complex which is initially in conformer III. Since species **O**(III) is presumed to convert to **R**(V) upon reduction, three possible pathways exist, each involving two intermediate species for which the conformers are designated in parentheses: (i) **O**(III) ⇌ **Y**(III) ⇌ **Z**(II) ⇌ **R**(V), (ii) **O**(III) ⇌ **W**(II) ⇌ **Z**(II) ⇌ **R**(V), (iii) **O**(III) ⇌ **W**(II) ⇌ **X**(V) ⇌ **R**(V). (Atom representations are identical to those in Fig. 2.)

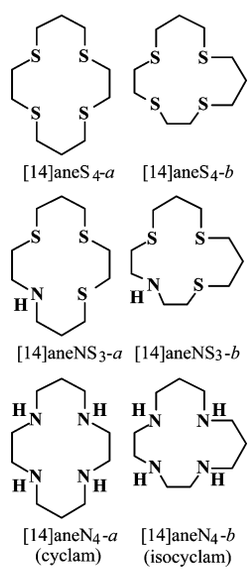

Fig. 4 Ligands discussed in the current study.

the ligand was in conformer II;[24] and only two Cu(II) crystal structures have been reported in which 5,6,5,6 macrocycles are in conformer II, *viz.*, (i) the blue (unstable) form of Cu^{II}(tet-*a*)[25] (tet-*a* = C-*meso*-5,5,7,12,12,14-hexamethyl-1,4,8,11-tetraazacyclotetradecane)—for which the crystal structure was not completely resolved—and (ii) the Cu(II) complex formed with the DL isomer of a derivative of [14]aneS$_4$-*a* in which the two ethylene bridges were replaced by *trans*-1,2-cyclohexane (designated as, DL-*trans,trans*-dicyhx-[14]aneS$_4$).[7] In the latter complex, the constraints imposed by the ring substituents appear to cause the ligand to prefer this unusual geometry. Significantly, the electron self-exchange rate constant representative of pathway B (Fig. 1) for this complex was larger than for any other copper system yet studied.[7]

An examination of prior work on macrocyclic tetramine

complexes suggested that conformer II might be readily generated for $Cu^{II}L$ complexes by reversing the position of one ethylene and one trimethylene bridge within the 14-membered macrocycle to produce a 5,5,6,6 sequence of chelate rings. Previously reported crystal structures on complexes of 1,4,7,11-tetraazacyclotetradecane (isocyclam or [14]aneN$_4$-*b*) (Fig. 4), with Ni(II),[26,27] Cu(II)[28,29] and Zn(II)[30] have shown that, in all cases, the ligand is in conformer II, presumably due to the specific strains imposed upon the bond torsion angles.[31] Unfortunately, the redox potentials for the Cu(II/I) complexes with cyclam and isocyclam are too negative to facilitate comparative electron-transfer kinetic studies.[32] However, the corresponding S_4 and NS_3 complexes have much more positive potentials[23] so that the Cu(I) complexes can easily be generated.

In the current work we have synthesized for the first time the S_4 and NS_3 macrocycles with the 5,5,6,6 chelate ring sequence, *viz.*, 1,4,7,11-tetrathiacyclotetradecane ([14]aneS$_4$-*b*)[33] and 1,7,11-triathia-4-azacyclotetradecane([14]aneNS$_3$-*b*)(Fig.4). We have determined the crystal structure for [Cu^{II}([14]aneNS$_3$-*b*)-(H_2O)](ClO_4)$_2$ to confirm that the coordinated ligand preferentially adopts conformer II. We have then determined the following properties of the complexes formed by copper with both [14]aneS$_4$-*b* and [14]aneNS$_3$-*b* in aqueous solution: (i) the $Cu^{II}L$ and $Cu^{I}L$ stability constants, (ii) the $Cu^{II}L$ complex formation and dissociation rate constants, (iii) the $Cu^{II/I}L$ redox potentials and (iv) the $Cu^{II/I}L$ electron-transfer kinetics. We have previously determined these same properties for $Cu^{II/I}$-([14]aneS$_4$-*a*);[1,34–36] and the first three properties have been reported earlier by us for $Cu^{II/I}$([14]aneNS$_3$-*a*) (*i.e.*, 1,4,8-trithia-11-azacyclotetradecane).[23,37] To complete the data acquisition, the electron-transfer kinetics for the latter system were studied as part of the current work. The specific behavior of the two pairs of corresponding systems involving the two different chelate ring sequences are compared and the differences interpreted in terms of the relative impact of the donor atom inversion steps on $Cu^{II}L$ complex dissociation and on the Cu(II/I) electron-transfer process.

Experimental

Ligand syntheses

The generalized synthetic, separation and characterization techniques used in our laboratories for the preparation of macrocyclic thiaether ligands have been previously described in detail.[38] The specific syntheses of [14]aneS$_4$-*a*[39] and [14]aneNS$_3$-*a*[40] have also been previously described. Synthetic schemes for the *b* isomers are presented here for the first time.

Synthetic scheme for [14]aneS$_4$-*b*

Our generalized high-dilution macrocyclization technique was utilized in anhydrous DMF containing finely milled anhydrous K_2CO_3 for the synthesis of [14]aneS$_4$-*b*. A 0.1 mol scale condensation of 2-mercaptoethyl sulfide (Aldrich Chemical Co.) with bis(3-chloropropyl) sulfide was carried out at 70 °C over a 5-h period. (**CAUTION:** *Bis(3-chloropropyl) sulfide is a vesicant and should be handled with extreme care!*) The latter synthon was prepared by reaction of 3,3′-thiodipropanol (Aldrich Chemical Co.) with thionyl chloride in methylene chloride and used in crude form after Kugelrohr evaporation of solvent below 40 °C/0.05 Torr. Flash chromatography of the washed, concentrated cyclization residue with 5:95 toluene–cyclohexane afforded 13.9 g (51.7%) of the crude product. The latter exhibited R_f = 0.55 when developed with 5:95 actetate–toluene on MK6F Whatman glass TLC plates. The crude [14]aneS$_4$-*b* was further purified by charcoal treatment and recrystallized from ethanol: mp = 94–96 °C, 19.7 g (79.9%). ^{13}C NMR (20.15 MHz, $CDCl_3$), δ in ppm (multiplicity): 30.18, 30.52, 31.58, 31.96, 32.08. FT-IR (KBr neat), in cm^{-1} (relative intensity): 2916 (w), 2823 (s), 1423 (m), 1253 (w), 1239 (w), 1189 (w), 1133 (w), 1034 (w), 762 (w); EI-MS, *m*/*z* (relative intensity): 268 M^+ (62), 207 (18), 181 (20), 106 (100), 74 (38), 133 (20).

Synthetic scheme for [14]aneNS$_3$-*b*

The toluenesulfonamide precursor was prepared by the high-dilution macrocyclization technique in anhydrous DMF/K_2CO_3 on a 0.25 mol scale by condensation of 3-mercaptopropyl sulfide with bis(2-chloroethyl)-*N*-toluenesulfonamide. The 3-mercaptopropyl sulfide was prepared from 3,3′-thiodipropanol (Aldrich Chemical Co.) *via* the thiouronium procedure of Houk and Whitesides.[41]

The sulfonamide synthone was prepared by slow addition of 1.1 equivalents of *p*-toluenesulfonyl chloride to a cooled, 5–10 °C, 0.5 molar toluene solution of 1 : 1 diethanolamine–triethylamine. The reaction solution was washed twice with 10% HCl to remove unreacted amines, then with 5% NaOH, dried with $MgSO_4$, suction filtered and toluene rotary vacuum evaporated at 80 °C, 18 Torr, to yield a pale yellow oil of essentially pure product in greater than 80% yield. Without further purification the bis(2-hydroxyethyl)-*N*-toluenesulfonamide was reacted with 2.2 equivalents of thionyl chloride in a 0.3 molar methylene chloride solution to form the bis(2-chloroethyl)-*N*-toluenesulfonamide. After rotary vacuum evaporation of methylene chloride at 30 °C, 18 Torr, followed by Kugelrohr evaporation at 30 °C, 0.05 Torr, the resulting dark yellow oil was used in the macrocyclization without further purification. Macrocyclization by the procedure used for the isomeric 1,4,8-trithia-11-azacylotetradecane-*N*-toluenesulfonamide[40] afforded the 1,7,11-trithia-4-azacyclotetradecane-*N*-toluenesulfonamide in 28% yield after elution column chromatography, 30 : 70 cyclohexane–toluene, and recrystallization from 60 : 40 cyclohexane–toluene, mp = 130–135 °C. Detosylation by the identical procedure employed for 1,4,8-trithia-11-azacyclotetradecane ([14]aneNS$_3$-*a*)[40] afforded the free amine ([14]aneNS$_3$-*b*) from a 0.08 mol scale reaction in 59% yield as colorless crystals from hexane: mp = 46–47 °C. ^{13}C NMR (20.15 MHz, $CDCl_3$), δ in ppm: 28.50, 29.58, 30.19, 30.32, 30.54, 31.08, 31.41, 32.59, 46.73, 49.88. FT-IR (KBr neat), in cm^{-1} (relative intensity): 3276 (s), 2940 (s), 2805 (s), 2664 (m), 1429 (s), 1287 (s), 1142 (w), 1111 (m), 997 (m), 750 (m). EI-MS, *m*/*z* (relative intensity): 250 M^+ (80), 59 (41).

Other reagents

Copper perchlorate and sodium perchlorate were prepared by adding $HClO_4$ to $CuCO_3$ and Na_2CO_3, respectively, as previously described.[42] (**CAUTION:** *Perchlorate salts are potentially explosive and should be handled with care in small quantities. They should never be heated to dryness!*) The preparative methods utilized for all counter reagents have been previously reported.[1]

Crystal structure

A crystal of [Cu^{II}([14]aneNS$_3$-*b*)(H_2O)](ClO_4)$_2$ was grown by evaporation from an aqueous solution containing a large excess of Cu(ClO_4)$_2$. Diffraction data were collected on a Siemens/Bruker P4/CCD diffractometer equipped with monochromated Mo-Kα radiation and the manufacturer's SMART collection software and SAINT processing software. A hemisphere of data was collected at 10 s frame^{-1} with 0.3° between each frame. Absorption corrections were applied with the program SADABS.[43] The structure was solved and refined on F^2 with the programs SHELXS and SHELXL-93.[43] Hydrogen atoms were placed in calculated or observed positions. All non-hydrogen atoms were anisotropically refined. Typical perchlorate disorder is evident in the large thermal parameters. Perchlorates labeled Cl(1) and Cl(2) occupy crystallographic 2-fold axes.

CCDC reference number 192149.

See http://www.rsc.org/suppdata/dt/b3/b300602f/ for crystallographic data in CIF or other electronic format.

Instrumentation

Scans of the UV-visible spectra were obtained using a Hewlett-Packard Model 8452A spectrophotometer. Precise molar absorptivity and stability constant values were measured using a Cary Model 17D dual-beam spectrophotometer. All pH measurements were made with either an Orion Model 901 Microprocessor Ionalyzer or an Orion Model 720A pH meter. Cyclic voltammograms were measured using a Bioanalytical Systems Electrochemical Analyzer, Model BAS 100 (BAS, West Lafayette, IN). All potential measurements were referenced to ferroin in 0.05 M KCl ($E^{0'}$ = 1.117 V)[44] as an external standard. All kinetic measurements were made with a Durrum D110 stopped-flow spectrophotometer with Kel-F fittings, equipped with air-tight syringes, which was interfaced to a PC. For both the thermodynamic and kinetic measurements, the temperature was thermostatted at 25.0 ± 0.2 °C.

Solutions for kinetic and thermodynamic measurements

All solutions were prepared using conductivity-grade distilled-deionized water. The macrocyclic ligands were dissolved in solutions containing a large excess of $Cu(ClO_4)_2$. Ligand concentrations were determined by a mole-ratio displacement plot in which the decrease in the intense S-to-Cu charge-transfer band (≈390 nm) was monitored as increments of a standard Hg(II) solution were added. The point at which the absorbance reached zero was taken as the equivalence point. Solutions of Cu^{I}([14]aneS$_4$-*b*) were prepared by adding copper shot to standardized $Cu^{II}L$ solutions and letting them sit under a nitrogen atmosphere with stirring for about two hours: $Cu^0 + 2Cu^{II}L \longrightarrow Cu^{II} + 2Cu^{I}L$. Due to their lower potential values, Cu^{I}([14]aneNS$_3$-*a*) and Cu^{I}([14]aneNS$_3$-*b*) were prepared by controlled potential electrolysis of the standard Cu(II) solutions: $Cu^{II}L + e^- \longrightarrow Cu^{I}L$. In all cases, the solutions were completely bleached, indicating that the reactions were quantitative so that the resulting $Cu^{I}L$ concentrations were presumed to be equal to that of the initial $Cu^{II}L$ solutions. The conditional stability constants and the complex formation and dissociation rate constants for the copper complexes of [14]aneNS$_3$-*a* and [14]aneNS$_3$-*b* were pH dependent. The pH of solutions used in these measurements was controlled by using our recently developed non-complexing buffers, specifically piperazine-*N*,*N*′-bis(3-propanesulfonic acid) (PIPPS: pK_a = 3.79) and piperazine-*N*,*N*′-bis(4-butanesulfonic acid) (PIPBS: pK_a = 4.29), which were synthesized as previously reported.[45,46] The concentrations of all counter reagent solutions were determined spectrophotometrically as described previously.[1] Ionic strength was maintained at 0.10 M in all solutions with $NaClO_4$.

Results

Crystal structure

The physical data for the crystal structure determination of $[Cu^{II}([14]aneNS_3\text{-}b)(H_2O)](ClO_4)_2$ are listed in Table 1. The principal bond lengths and angles associated with the copper coordination geometry are given in Table 2. An ORTEP drawing of the cationic unit is shown in Fig. 5. This structure shows that Cu(II) is five-coordinate with the unshared electron pairs on each of the sulfur donor atoms oriented in the same direction as the apically coordinated water molecule while the hydrogen attached to the nitrogen donor atom is oriented in the opposite direction to generate conformer II, consistent with the geometry previously reported for $[Cu^{II}([14]aneN_4\text{-}b)(NCS)]NCS$.[28]

Table 1 Crystal parameters and experimental data for X-ray diffraction measurements on $[Cu^{II}([14]aneNS_3\text{-}b)(H_2O)](ClO_4)_2$[a]

Parameter	$[Cu^{II}([14]aneNS_3\text{-}b)(H_2O)](ClO_4)_2$
Empirical formula	$CuC_{10}H_{23}NS_3Cl_2O_9$
Formula weight	531.91
Space group	*C*2
a/Å	13.7324(8)
b/Å	10.0394(5)
c/Å	14.6404(8)
α/°	90
β/°	95.122(1)
γ/°	90
V/Å^3	2010.3(2)
Z	4
D_c/g cm^{-3}	1.757
μ/mm^{-1}	1.706
$R(F)$[b]	0.0407
$R_w(F^2)$[c]	0.1096

[a] T = 295(2) K; λ = 0.71073 Å. [b] $R(F) = \Sigma||F_o| - |F_c||/\Sigma|F_o|$ for $2\sigma(I)$ reflections. [c] $R_w(F^2) = [\Sigma w(F_o^2 - F_c^2)^2/\Sigma w(F_o^2)^2]^{1/2}$ for $2\sigma(I)$ reflections.

Table 2 Selected bond lengths (Å) and bond angles (°) for the cationic unit in the crystal structure of $[Cu^{II}([14]aneNS_3\text{-}b)(H_2O)](ClO_4)_2$

Cu–S(1)	2.311(1)	Cu–S(3)	2.279(2)
Cu–S(2)	2.286(2)	Cu–N	2.004(4)
Cu displacement[a]	0.043(1)		
S(1)–Cu–S(2)	93.72(5)	S(2)–Cu–N	163.62(13)
S(2)–Cu–S(3)	95.68(5)	S(1)–Cu–O	84.46(11)
S(3)–Cu–N	86.53(13)	S(2)–Cu–O	98.75(12)
S(1)–Cu–N	87.16(12)	S(3)–Cu–O	84.60(11)
S(1)–Cu–S(3)	166.53(5)	N–Cu–O	97.6(2)

[a] Displacement of the Cu atom from the mean NS_3 plane toward the coordinated water molecule; the corresponding displacements for S(1), S(2), S(3) and N(1) are 0.260(1), −0.220(1), 0.256(1) and −0.296(1) Å, respectively.

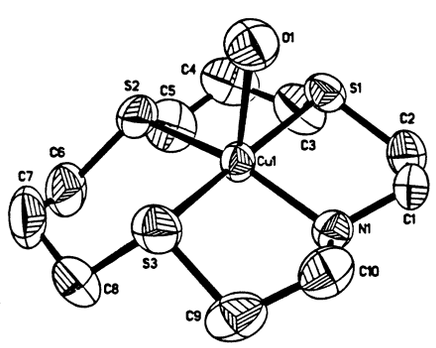

Fig. 5 ORTEP drawing of the cationic unit in the crystal structure of $[Cu^{II}([14]aneNS_3\text{-}b)(H_2O)](ClO_4)_2$ showing the atom numbering scheme. Hydrogen atoms have been omitted for clarity.

Ligand protonation constants

The titrimetric determination of the ligand protonation constant for [14]aneNS$_3$-*a* has been previously described.[37] The same approach was utilized for [14]aneNS$_3$-*b* in this study. For the latter determination, perchloric acid was added to a 0.10 mM solution of ligand to adjust the pH to approximately 3.0 and the solution was then titrated with standard NaOH to pH 10.5. The PKAS software developed by Martell and Motekaitis[47] was used as previously noted[45,46] to calculate the optimal value of the mixed-mode protonation constant defined as:

$$K_H^{\ m} = \frac{[HL^+]}{a_H[L]} \quad (1)$$

Table 3 Physical parameters for copper(II) complexes with [14]aneS$_4$-*a*, [14]aneS$_4$-*b*, [14]aneNS$_3$-*a* and [14]aneNS$_3$-*b* in aqueous solution at 25 °C, $\mu = 0.10$ M (ClO_4^-)

Complexed ligand	E^f/V *vs.* SHE	λ_{max}/nm	$10^{-3}\varepsilon_{Cu^{II}L}$/M^{-1} cm^{-1}	log K_{H^-}	log $K_{Cu^{II}L}$	log $K_{Cu^{I}L}$ (calc.)
[14]aneS$_4$-*a*	0.59[a]	390[b]	8.0[b]	n.a.	4.34[b]	12.1[a]
[14]aneS$_4$-*b*	0.69[c]	411[c]	8.3[c]	n.a.	2.74(7)[c]	12.2[c]
[14]aneNS$_3$-*a*	0.38[d]	365[e]	7.7[e]	8.75[e]	9.25[e]	13.6[d]
[14]aneNS$_3$-*b*	0.41[c]	378[c]	8.2[c]	8.2(1)[c]	8.34(4)[c]	13.1[c]

[a] Ref. 36. [b] Ref. 34. [c] This work; digits in parentheses represent the standard deviation for the last digit shown (*e.g.*, 2.74(7) denotes 2.74 ± 0.07). [d] Ref. 23. [e] Ref. 37.

where a_H represents the activity of solvated hydrogen ion. The resulting K_H^m value is listed in Table 3.

Spectra and stability constants

As previously reported for the Cu(II) complexes with [14]aneS$_4$-*a* [34] and [14]aneNS$_3$-*a*,[37] the corresponding complexes formed with [14]aneS$_4$-*b* and [14]aneNS$_3$-*b* exhibit strong S⟶Cu charge-transfer bands in the visible region. The molar absorptivity value of each Cu^{II}L complex and the corresponding conditional stability constant, $K_{Cu^{II}L}'$, for each of the latter complexes were determined simultaneously using the McConnell-Davidson approach.[34,38,48] In eqn. (2),

$$Cu^{II} + L' \rightleftharpoons Cu^{II}L \quad K_{Cu^{II}L}' \tag{2}$$

L′ represents the total uncomplexed ligand, which, in the case of the [14]aneNS$_3$ ligands, includes both the unprotonated and protonated species. For Cu^{II}([14]aneNS$_3$-*b*), the measurements were carried out at pH 3.77 using a total ligand concentration of 28 μM while the total Cu(II) concentration was varied from 93 to 280 μM to yield a conditional stability constant value of $K_{Cu^{II}L}' = (8.25 \pm 0.09) \times 10^3$ M^{-1}. Our past studies with acyclic polythiaethers [49] have amply demonstrated that the Cu(II)-polythiaether complexes are exceptionally weak in aqueous solution in the absence of complete coordination by a quadridentate macrocycle. Based on these prior observations, it is presumed that the protonated complex with [14]aneNS$_3$, Cu^{II}HL, is not a stable species under the conditions used in the current work. Therefore, the conditional stability constant represents only the Cu^{II}L species from which we can calculate the corrected thermodynamic stability constant based solely on the ligand protonation constant:

$$K_{Cu^{II}L} = \frac{[Cu^{II}L]}{[Cu^{II}][L]} = \frac{[Cu^{II}L]}{[Cu^{II}]\alpha_L[L']} = \frac{K_{Cu^{II}L}'}{\alpha_L} \tag{3}$$

$$\alpha_L = \frac{[L]}{[L] + [HL^+]} = \frac{1}{1 + K_H^m a_H} \tag{4}$$

where a_L is unity for [14]aneS$_4$-*b* and 3.80×10^{-5} at pH 3.77 for [14]aneNS$_3$-*b*. The wavelength of maximum absorbance, the corresponding molar absorptivity value, and the stability constant for each of the four Cu(II) complexes are listed in Table 3.

Copper(II/I) complex potentials and copper(I) complex stabilities

The potential values for Cu$^{II/I}$([14]aneS$_4$-*a*)[36] and Cu$^{II/I}$([14]aneNS$_3$-*a*)[23] have been previously reported. Slow scan cyclic voltammograms (v = 10–100 mV s^{-1}) were essentially reversible for solutions containing [14]aneS$_4$-*b* and [14]aneNS$_3$-*b* in the presence of excess Cu(II). As noted in the Experimental section, the potential values were calibrated against ferroin in 0.05 M KCl as an external standard. For each of the latter systems, the $E_{1/2}$ value was presumed to represent the formal potential as listed in Table 3.

The measured potential values for the Cu$^{II/I}$L systems were combined with the stability constants determined for the Cu^{II}L complexes to permit the Cu^{I}L stability constants to be calculated from the Nernst relationship:

$$E^f = E_{aq}^{0'} - \frac{2.303RT}{nF} \log \frac{K_{Cu^{II}L}}{K_{Cu^{I}L}} \tag{5}$$

where $E_{aq}^{0'}$ represents the concentration potential for the aquated Cu(II/I) redox couple (0.13 V)[50] and the other terms retain their usual significance. The resulting $K_{Cu^{I}L}$ values are included in Table 3.

Complex formation kinetics

The formation rate constants for each of the *b*-isomer complexes were determined by mixing excess aquated Cu(II) ion with ligand in a stopped-flow spectrophotometer and monitoring the appearance of the product, Cu^{II}L:

$$Cu^{2+} + L' \underset{k_d}{\overset{k_f}{\rightleftharpoons}} Cu^{II}L \tag{6}$$

Due to the very limited aqueous solubility of [14]aneS$_4$-*a*, the formation rate constant for Cu^{II}([14]aneS$_4$-*a*) was originally obtained by measuring the rate of formation in a series of methanol–water mixtures and extrapolating to aqueous conditions.[35] This value was later corroborated from the product of the aqueous dissociation rate constant and complex stability constant.[42] In the current work, the Cu^{II}([14]aneS$_4$-*b*) complex formation rate constant was measured directly in aqueous solution using a 10- to 50-fold excess of Cu(II) to yield observed pseudo-first-order rate constants in the range of 2×10^2 s^{-1}. As noted, the free ligand concentration was severely limited by its solubility (≈10 μM), thereby decreasing the sensitivity of the measurements; and the Cu(II) concentration could not be increased markedly due to the relative rapidity of this reaction. Under the conditions used, the reaction proceeded only to about 40% completion at the highest copper concentration used (0.5 mM). These limitations resulted in a large standard deviation for the resolved second-order formation rate constant: $k_{Cu}^L = (1.3 \pm 0.4) \times 10^5$ M^{-1} s^{-1}. However, this value was considered to be sufficiently accurate for our purposes since the same kinetic data generated a relatively precise dissociation rate constant of $k^{CuL} = (1.6 \pm 0.1) \times 10^2$ s^{-1} (obtained from the intercept of k_{obs}),[35] which, in turn, yielded a ratio of $k_{Cu}^L/k_{CuL} = 8.1 \times 10^2$, this latter value being within 25% of the stability constant obtained independently from equilibrium measurements. The formation rate constants for aquated Cu(II) reacting with both the unprotonated and protonated forms of [14]aneNS$_3$-*a* were determined previously from a kinetic study at variable pH in aqueous media.[37] A similar approach was used for Cu^{II}([14]aneNS$_3$-*b*) by determining the trend in the apparent formation rate constant over the range of pH 2.5–4.5, using our recently developed non-complexing buffers.[45,46] The specific complex formation rate constants for both the unprotonated (k_{Cu}^L) and protonated (k_{Cu}^{HL}) ligand species were then resolved according to the relationship:[37,51]

Table 4 Specific formation rate constants for the reaction of aquocopper(II) ion with [14]aneS$_4$-*a*, [14]aneS$_4$-*b*, [14]aneNS$_3$-*a* and [14]aneNS$_3$-*b* at 25 °C, $\mu = 0.1$ M (ClO_4^-)

Ligand reacted	$10^{-5}k_{Cu}^{L}$/M^{-1} s^{-1}	$10^{-2}k_{Cu}^{HL}$/M^{-1} s^{-1}	k^{Cu-L} (calc.)/s^{-1}
[14]aneS$_4$-*a*	1.3 [a]	n.a.	0.18×10^2 [b]
[14]aneS$_4$-*b*	1.3(4) [c]	n.a.	2.4×10^2, [e] $1.6(1) \times 10^2$ [c,f]
[14]aneNS$_3$-*a*	32 [d]	1.4 [d]	0.18×10^{-2} [e]
[14]aneNS$_3$-*b*	28(3) [c]	≈2.4 [c]	1.1×10^{-2} [e]

[a] Extrapolated to aqueous solution from formation kinetics measured in methanol–water mixtures: ref. 36. [b] Measured directly in aqueous solution using Hg(II) ion as a scavenger: ref. 42. [c] This work; digits in parentheses are standard deviations (see Table 3). [d] Ref. 35. [e] Calculated from $K_{Cu}II_L$ and k_{Cu}^{L}. [f] Determined experimentally as the intercept in the plot of k_{obs} *vs.* [Cu^{2+}] (see ref. 35: eqn (7) and Fig. 3).

Table 5 Electron-transfer rate constants for $Cu^{II/I}L$ systems reacting with selected counter reagents in aqueous solution at 25 °C, $\mu = 0.10$ M

Reagent [a]	$10^{-5}k_{12}$ (or k_{21})/M^{-1} s^{-1}			
	$Cu^{II/I}$([14]aneS$_4$-*a*) [b]	$Cu^{II/I}$([14]aneS$_4$-*b*)	$Cu^{II/I}$([14]aneNS$_3$-*a*)	$Cu^{II/I}$([14]aneNS$_3$-*b*)
Reductants				
$Co^{II}(TIM)(H_2O)_2$	0.000075(4)			
$Ru^{II}(NH_3)_4(bpy)$	4.80(4)	5.4(2)		
$Ru^{II}(NH_3)_5(isn)$	19(3)	50(10)	0.021(1), [c] 0.024(2) [d]	0.088(1), [c] 0.127(6), [c] 0.16(1), [d] 0.129(9) [d]
$Ru^{II}(NH_3)_5(py)$	45(3)		0.134(8), [c] 0.126 [d]	0.30(2), [c] 0.46(1) [d]
Oxidants				
$Ru^{III}(NH_3)_4(bpy)$	0.98(3)		0.51(4) [c], 0.98(6) [d]	2.0 (6), [c] 5.2(4) [d]
$Ru^{III}(NH_3)_4(phen)$			0.27(2), [c] 0.15(1) [d]	5.6(3), [c] 6.2(2) [d]
$Ni^{III}([14]aneN_4)(H_2O)_2$	4.5(4)	4.0(4), 5.2(6)		
$Ru^{III}(NH_3)_2(bpy)_2$	20(10)	$\approx 5 \times 10^2$ [e]		*Too fast to follow*
$Fe^{III}(4,7\text{-dmphen})_3$	72(24)			

[a] The potentials, self-exchange rate constants and ion size parameters for all reagents are tabulated in ref. 2. [b] Ref. 2. [c] pH ≈ 3.0 controlled with PIPPS buffer. [d] pH ≈ 5.0 controlled with PIPBS buffer. [e] This reaction rate is extremely fast and only an approximate rate constant could be obtained.

$$k_f[Cu^{2+}][L'] = k_{Cu}^{L}[Cu^{2+}][L] + k_{Cu}^{HL}[Cu^{2+}][HL^+]$$

or

$$k_f/a_L = k_{Cu}^{L} + K_H^{m}a_H k_{Cu}^{HL} \quad (7)$$

The resolved formation rate constants for all four Cu(II) complexes are listed in Table 4. This table also includes the values for the apparent proton-independent dissociation rate constant, k^{Cu-L}, as calculated from the relationship:

$$k^{Cu-L} = k_{Cu}^{L}/K_{Cu^{II}L} \quad (8)$$

Electron-transfer kinetics

The electron-transfer kinetics for the reaction of $Cu^{II/I}$([14]aneS$_4$-*a*) with eight different counter reagents have been previously reported.[1] For each of the other three systems considered in this work, the electron-transfer kinetics were studied with two reductants (A_{Red}) and two oxidants (A_{Ox}) as counter reagents:

$$Cu^{II}L + A_{Red} \underset{k_{21}}{\overset{k_{12}}{\rightleftharpoons}} Cu^{I}L + A_{Ox} \quad (9)$$

The resolved cross-reaction rate constants, k_{12} and k_{21}, are listed in Table 5.

For the systems involving the two NS_3 ligands, the electron-transfer kinetics were studied at two different pH values, 3.0 and 5.0, to determine whether ligand protonation might be a factor in these reactions. The ruthenium reagents used in this work tend to be unstable at higher pH, giving rise to some uncertainty in the k_{12} and k_{21} values measured at pH 5.0. Thus, the discrepancies in some of the cross-reaction rate constant values for the two NS_3 systems at the two pH values are attributed largely to experimental error in the values obtained at the higher pH.

Discussion

Complex conformations

The crystal structure of [Cu^{II}([14]aneS$_4$-*a*)(ClO_4)$_2$] [22] has previously been determined to exist in conformer III (Fig. 2). This structure is consistent with structures reported for similar [14]aneN$_4$-*a* complexes with Cu(II) including [Cu^{II}([14]aneN$_4$-*a*)(H_2O)$_2$]F_2,[16] [Cu^{II}([14]aneN$_4$-*a*)(ClO_4)$_2$][15] and [Cu^{II}([14]aneN$_4$-*a*)Br_2];[17] and the same conformer is assumed to predominate for Cu^{II}([14]aneNS$_3$-*a*). By contrast, the crystal structure for [Cu^{II}([14]aneNS$_3$-*b*)H_2O](ClO_4)$_2$, as determined in the current work, reveals that the ligand is in conformer II with the nitrogen orienting its hydrogen toward the side of the macrocyclic ring opposite to the apical water molecule whereas the unshared electron pairs on the three sulfur donor atoms are directed toward the same side as the water molecule to generate conformer II. The same general conformer has been found previously in the crystal structures for [Cu^{II}([14]aneN$_4$-*b*)NCS]NCS [28] and [Zn^{II}([14]aneN$_4$-*b*)Cl]ClO_4.[30,52] In those cases, the nitrogen donor between the two ethylene bridges has its hydrogen oriented toward the apical ligand with the hydrogens on the other three nitrogens oriented toward the opposite side (that is, compared to Fig. 5, each donor atom in the [14]aneN$_4$-*b* complexes is oriented in the opposite direction relative to the apical ligand). The similarity of the structures for these [14]aneN$_4$-*b* complexes with that for Cu^{II}([14]aneNS$_3$-*b*) strongly supports the contention that the Cu^{II}([14]aneS$_4$-*b*) complex also preferentially adopts conformer II, although we have been unable to obtain a suitable crystal.

Relatively few crystal structures have been reported for Cu(I) complexes with macrocyclic ligands. The crystal structures of [Cu^{I}([14]aneS$_4$-*a*)]ClO_4 [53] and a related derivatized Cu(I) complex [6] proved to be polymeric. However, the electron-transfer kinetic data for these complexes showed no evidence of polymers in solution nor are such species likely to occur at the

low concentrations used in our studies. Our previous crystal structure of $[Cu^{I}([14]aneNS_3\text{-}a)]ClO_4$[23] showed the ligand to be in conformer V (Fig. 6) and the same conformer has also been found in the Cu(I) complexes formed with two substituted derivatives of [14]aneS$_4$-*a* in which one of the ethylene bridges was replaced either by *trans*-1,2-cyclohexane[4] or by *trans*-1,2-cyclopentane.[6] A related macrocyclic pentathiaether complex shows essentially the same structure.[54] Molecular mechanical calculations also support the premise that conformer V is the most stable conformation for monomeric Cu(I) complexes with 14-membered quadridentate ligands (*vide infra*). Thus, as indicated earlier, it is presumed that conformer V dominates for all of the Cu(I) complexes included in the current study.

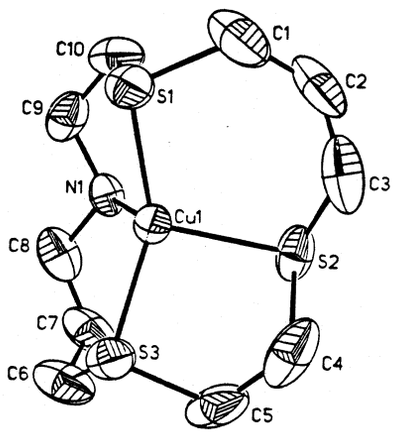

Fig. 6 ORTEP drawing of the cationic unit in the crystal structure of $[Cu^{I}([14]aneNS_3\text{-}a]ClO_4$ (from ref. 23) as a typical example of a reduced complex in conformer V. Hydrogen atoms have been omitted for clarity.

Physical parameters

The kinetic data in Table 4 show that the formation rate constants for the Cu(II) complexes are virtually identical for both of the S$_4$ complexes as well as for both of the NS$_3$ complexes. For the NS$_3$ complexes, the rate-determining step for complex formation is expected to be at the point of first-bond formation[37] and should, therefore, be uninfluenced by the chelate ring sequence.[55] For the S$_4$ macrocycles, the second-bond formation (ring closure) has been hypothesized to represent the rate-determining process, thereby accounting for the much smaller formation rate constants.[35] Although the strain involved in closing five- and six-membered chelate rings differs, the statistical probability of having the second-bond formation involve either a five- or a six-membered chelate ring is essentially identical for both the *a* and *b* macrocycles. Thus, as observed, the ring size sequence should have little influence on the formation rate constants.

In the last stage of complex formation with these macrocyclic ligands, the ligand must change from a folded (*cis*) to a planar (*trans*) complex.[37] Since this occurs after the rate-determining step, it is not reflected in the formation rate constants. As a corollary, however, an early step in complex *dissociation* must involve the change from a planar to a folded complex as an equilibrium step preceding the rate-determining step (Fig. 7).[56] The observation that the k^{Cu-L} values are larger for the complexes with the *b*-variant ligands suggests that they adopt the folded geometry much more readily.[27] Since molecular models make it apparent that conformer III (or I) must convert to conformer II before the complex can "fold" (Fig. 7),[56] the larger k^{Cu-L} values obtained for the *b* macrocyclic complexes represents supporting evidence for the hypothesis that these complexes preferentially adopt conformer II in solution (as well as in the crystalline state) since this conformer eliminates the initial nitrogen donor inversion step. However, we note that the increase in k^{Cu-L} is only seven-fold for the *b*-isomer complexes.

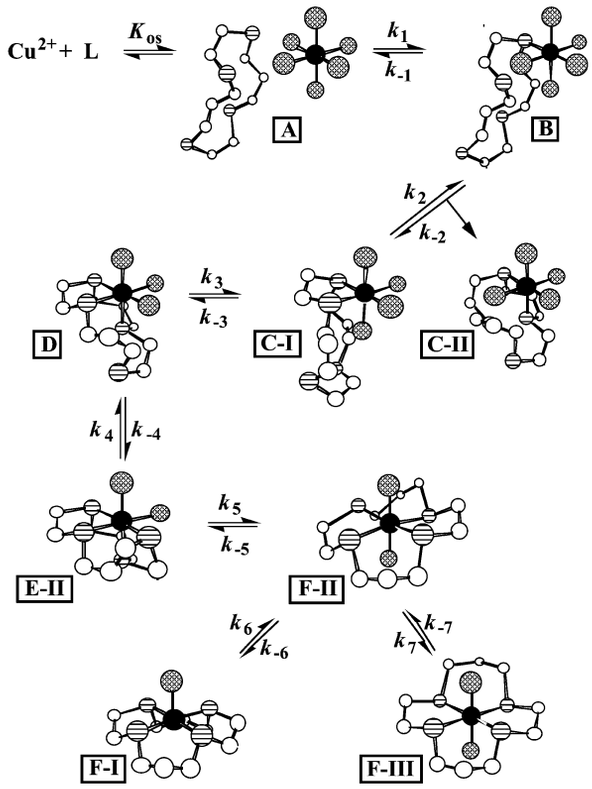

Fig. 7 Proposed scheme for the stepwise complex formation of aquocopper(II) ion reacting with a macrocyclic quadridentate ligand. Of the fully coordinated species, species E-II represents a folded complex and F-II, F-I and F-III are corresponding species in which all donor atoms are in the same plane. The first step in complex dissociation is either F-I ⟶ F-II or F-III ⟶ F-II which involves the inversion of one donor atom. (Atom designations are identical to those in Fig. 2.)

The foregoing interpretation is consistent with the work by Liang and Chung[57,58] on the rate of conversion of the blue isomer of Cu^{II}(tet-*a*) (*vide supra*), which is known to represent conformer II,[25] to the more stable red isomer, which exists in conformer III. However, in those studies, a nitrogen donor atom must undergo inversion and the need to abstract a hydrogen atom from the inverting nitrogen[56] vastly slows the rate of conformational change as is evident from the pH dependence. Although our two pairs of ligands may exhibit different levels of strain for conformer II (due to the differences in their chelate ring sequences), the relatively small difference in the k^{Cu-L} values suggests that the energy barrier involved in the initial conformer III ⟶ conformer II inversion step for the *a* ligands is also relatively small.

Electron self-exchange rate constants

Each of the cross-reaction rate constant values (k_{12} and k_{21}) in Table 5 were used to generate values for the apparent electron self-exchange rate constant, k_{11},

$$*Cu(II) + Cu(I) \underset{}{\overset{k_{11}}{\rightleftharpoons}} *Cu(II) + Cu(I) \qquad (10)$$

by means of the Marcus cross relationship:[59]

$$k_{11} = \frac{(k_{12})^2}{k_{22}K_{12}f_{12}(W_{12})^2} \text{ or } k_{11} = \frac{(k_{21})^2}{k_{22}K_{21}f_{21}(W_{21})^2} \qquad (11)$$

where k_{22} represents the self-exchange rate constant for the counter reagent; K_{12} and K_{21} represent the equilibrium constants for the overall reactions as calculated from the redox potentials; f_{12} and f_{21} represent non-linear terms calculated from

Table 6 Electron self-exchange rate constants for $Cu^{II/I}L$ systems as determined with various counter reagents in aqueous solution at 25 °C, $\mu = 0.10$ M

Reagent	log k_{11}/M^{-1} s^{-1}			
	$Cu^{II/I}$([14]aneS$_4$-*a*)[a]	$Cu^{II/I}$([14]aneS$_4$-*b*)	$Cu^{II/I}$([14]aneNS$_3$-*a*)	$Cu^{II/I}$([14]aneNS$_3$-*b*)
Reductants				
$Co^{II}(TIM)(H_2O)_2$	3.42			
$Ru^{II}(NH_3)_4$(bpy)	3.79	2.2		
$Ru^{II}(NH_3)_5$(isn)	4.02	2.9	1.47,[b] 1.59[c]	2.21,[b] 2.53,[b] 2.71,[c] 2.54[c]
$Ru^{II}(NH_3)_5$(py)	3.89		1.74,[b] 1.69[c]	1.96,[b] 2.34[c]
Oxidants				
$Ru^{III}(NH_3)_4$(bpy)	2.58[d]		0.31,[b] 0.88[c]	1.98,[b] 2.81[c]
$Ru^{III}(NH_3)_4$(phen)			1.59,[b] 1.05[c]	2.68,[b] 2.78[c]
Ni^{III}([14]aneN$_4$)$(H_2O)_2$	2.44[d]	2.92, 3.16		
$Ru^{III}(NH_3)_2(bpy)_2$	0.1	≈ 3.1–4.9[e]		
Fe^{III}(4,7-dmphen)$_3$	−0.1			

[a] Ref. 2. [b] pH ≈ 3.1 controlled with PIPPS buffer. [c] pH ≈ 5.0 controlled with PIPBS buffer. [d] The oxidation of Cu^{I}([14]aneS$_4$-*a* by $Ru^{III}(NH_3)_4$(bpy) and Ni^{III}([14]aneN$_4$) showed evidence of gating (see ref. 2). [e] The very large experimental second-order rate constants for this reaction (approaching 10^8 M^{-1} s^{-1}) resulted in a large uncertainty in the calculated k_{11} values for the Cu(II/I) complex.

the other parameters; and W_{12} and W_{21} represent electrostatic work term corrections.[1]

As noted in the Introduction, our earlier studies on $Cu^{II/I}$-([14]aneS$_4$-*a*)[1] and related systems,[2–7,60] have shown that their electron-transfer kinetic behavior is consistent with a mechanistic scheme in which a major conformational change and the electron-transfer step occur sequentially rather than concertedly to yield at least two competing pathways, A and B, (Fig. 1). For most of the systems studied to date, the overall behavior indicates that pathway A is preferred, implying that intermediate **P** is more stable than **Q**. As the driving force of the oxidation reaction is increased—by (i) increasing the potential differences between the reactants, (ii) increasing the self-exchange rate constant of the counter reagent, or (iii) increasing the concentration of the counter reagent—it is possible to reach a point where the electron-transfer rate exceeds the rate of the conformational change itself (**R** ⟶ **P**). Under these circumstances, the first-order conformational change may become rate determining so that the oxidation reaction rate *via* pathway A cannot be increased further and the reaction is said to be "gated".[61] As the driving force is increased further, the reaction ultimately switches to pathway B as shown by the markedly smaller k_{11} values for $Cu^{II/I}$([14]aneS$_4$-*a*) reacting with the two strongest oxidants, $Ru^{III}(NH_3)_2(bpy)_2$ and Fe^{III}(4,7-dmphen)$_3$ (Table 6).

Kinetic implications of comparative k_{11} values

For each of the three Cu(II/I) systems for which the electron-transfer kinetics were determined in this study, the k_{11} values calculated from all oxidation and reduction reactions are considered to be consistent within experimental error (Table 6). This indicates that all reactions are proceeding by the dominant pathway which, based on our earlier studies, is presumed to be pathway A. It is particularly interesting to note that, for the $Cu^{II/I}$([14]aneS$_4$-*b*) system, the second-order rate constant for the oxidation of Cu^{I}([14]aneS$_4$-*b*) with $Ru^{III}(NH_3)_2(bpy)_2$ approached 10^8 M^{-1} s^{-1} without showing any indication of rate-limiting behavior attributable to ligand conformational change. This suggests that the **R** ⟶ **P** transformation is exceptionally rapid with this system.[62]

In a recent comparative study on eight closely related $Cu^{II/I}L$ systems, including $Cu^{II/I}$([14]aneS$_4$-*a*), under conditions where both pathway A and pathway B (Fig. 1) were evaluated, we observed a variation of nearly 10^6 among the 16 individual self-exchange rate constant values, k_{11}.[7] However, resolution of the rate constants for the specific Cu(II/I) electron-transfer steps (horizontal reactions in Fig. 1) ***O** + **P** ⇌ ***P** + **O** and ***Q** + **R** ⇌ ***R** + **Q** revealed that 13 of the 16 values were within the range of 10^5–10^6 M^{-1} s^{-1}—that is, within a factor of ten—a variation which is generally conceded to represent the experimental limits for reproducing such values when utilizing various reagents. If we assume that the rate constant for the electron-transfer step is within this same range (*i.e.*, 10^5–10^6 M^{-1} s^{-1}) for the systems included in the current study, then the deviations of the resolved k_{11} values from this range should reflect the magnitude of the reorganizational energy involved in the ligand conformational changes.

As noted in the Introduction, the ligand conformational change (*via* either pathway A or B) should involve the inversion of two coordinated sulfur donor atoms for a system in which the $Cu^{II}L$ complex exists predominantly in either conformer I or conformer III,[13] but only one donor atom is required to invert for a system in which the stable $Cu^{II}L$ complex is in conformer II. Thus, our initial premise was that the systems involving the *b* isomers should undergo more rapid overall electron transfer if the reorganizational barrier for the III ⇌ II (or I ⇌ II) conformational change were significant. For the two NS_3 ligands, the k_{11} value for $Cu^{II/I}$([14]aneNS$_3$-*b*) is essentially 10-fold larger than for $Cu^{II/I}$([14]aneNS$_3$-*a*). Although this difference is not large, we note that it closely parallels the difference in the two dissociation rate constants, which was earlier attributed to the fact that the *a* isomer had to undergo an extra donor atom inversion in the first stage of the dissociation process, presumably representing conformer III ⇌ conformer II. However, the two S_4 ligand complexes show the opposite trend, at least insofar as the reduction reactions are concerned. Since the k_{11} values for the Cu(II/I) systems with the two *b* isomers are virtually identical, it appears that the k_{11} value for $Cu^{II/I}$([14]aneS$_4$-*a*) is anomalously large in this series. This result was entirely unexpected and is difficult to rationalize.

We have attempted to generate approximate molecular mechanical calculations for each of the dominant conformers for all four $Cu^{II}L$ and $Cu^{I}L$ complexes. Several approaches have been tried and none are entirely satisfactory since the Cu–S force constants, in particular, are not known. However, we have found that a reasonably consistent set of relative strain energies can be generated using Chem3D Plus. In this approach it is assumed that, since the same type of bonds are involved in all four systems, the relative magnitude of the residuals which remain upon strain minimization reflects the relative strain existing within the conformer. As listed in Table 7, these qualitative values indicate that conformers I, II and III are much more stable than conformer V for the $Cu^{II}L$ complexes. (In making comparisons, it should be noted that the calculations are not sufficiently precise to distinguish between the relative stabilities of conformers I, II and III for the $Cu^{II}L$

Table 7 Summary of residual strain energies for copper(II) and copper(I) complexes with [14]aneS$_4$-*a*, [14]aneS$_4$-*b*, [14]aneNS$_3$-*a* and [14]aneNS$_3$-*b*

		Conf I	Conf IIA[a]	Conf IIB[b]	Conf IIC[c]	Conf III	Conf V
Copper(II)							
	[14]aneS$_4$-*a*	3.08	9.11	–	–	4.53	24.93
	[14]aneS$_4$-*b*	4.78	14.18[a]	10.12[b]	10.81[c]	9.56	27.10
	[14]aneNS$_3$-*a*	4.90	6.40[d]	8.84[e]	9.88[f]	5.35	NO[g]
	[14]aneNS3-*b*	7.01	9.97[a]	8.03[b]	13.04[c]	7.56	NO[g]
Copper(I)							
	[14]aneS$_4$-*a*	43.29	32.10	–	–	62.65	16.72
	[14]aneS$_4$-*b*	39.49	24.44[a]	28.70[b]	33.48[c]	NO[g]	16.02
	[14]aneNS$_3$-*a*	41.19	27.49[d]	28.93[e]	21.01[f]	56.94	14.51
	[14]aneNS$_3$-*b*	44.26	25.7[a]	31.08[b]	24.01[c]	NO[g]	15.98

[a] For the [14]aneS$_4$-*b* and [14]aneNS$_3$-*b* complexes, the unique donor atom in Conf IIA is the one adjacent to the 5,5 linkages (*i.e.*, N in the case of [14]aneNS$_3$-*b*). [b] For the [14]aneS$_4$-*b* and [14]aneNS$_3$-*b* complexes, the unique donor atom in Conf IIB is the sulfur adjacent to the 5,6 linkages. [c] For the [14]aneS$_4$-*b* and [14]aneNS$_3$-*b* complexes, the unique donor atom in Conf IIC is the sulfur adjacent to the 6,6 linkages. [d] For the [14]aneNS$_3$-*a* complexes, the unique donor atom in Conf IIA is nitrogen. [e] For the [14]aneNS$_3$-*a* complexes, the unique donor atom in Conf IIB is the sulfur closest to the nitrogen. [f] For the [14]aneNS$_3$-*a* complexes, the unique donor atom in Conf IIC is the sulfur furthest from the nitrogen. [g] The strain energies for these conformers could not be minimized.

species.) In fact, for the two NS$_3$ ligands, the oxidized complexes could not be minimized in conformer V without "freezing" the positions of three or more atoms. The data also support the premise that conformer V is the most stable geometry for the Cu^{I}L species and conformer II appears to be much more stable than either conformer I or III for these reduced species.

All of the kinetic data obtained in this study, in conjunction with the qualitative molecular mechanical calculations are consistent with our earlier postulate[13] that the II $\rightleftharpoons$ V interconversion represents the discrete conformational step during the overall electron-transfer reaction, that is, the latter conformational change is presumed to represent the dominant energy barrier for both vertical steps in Fig. 1. This implies that, in the case of the Cu(II/I) systems involving the *a* isomers, species **O** represents the (rapidly) equilibrated mixture of conformers III (or I) and II, and intermediates **P** and **Q** represent conformers II and V, respectively. The apparently anomalous behavior of the system involving [14]aneS$_4$-*a* may be attributable to a smaller barrier in the II $\rightleftharpoons$ V conformational change, but this hypothesis cannot be confirmed on the basis of data currently available.

Acknowledgements

This work was supported by the US National Science Foundation under Grants CHE-9528831 and CHE-9817919.

References and notes

1 N. E. Meagher, K. L. Juntunen, C. A. Salhi, L. A. Ochrymowycz and D. B. Rorabacher, *J. Am. Chem. Soc.*, 1992, **114**, 10411–10420.
2 N. E. Meagher, K. L. Juntunen, M. J. Heeg, C. A. Salhi, B. C. Dunn, L. A. Ochrymowycz and D. B. Rorabacher, *Inorg. Chem.*, 1994, **33**, 670–679.
3 B. C. Dunn, L. A. Ochrymowycz and D. B. Rorabacher, *Inorg. Chem.*, 1995, **34**, 1954–1956.
4 C. A. Salhi, Q. Yu, M. J. Heeg, N. M. Villeneuve, K. L. Juntunen, R. R. Schroeder, L. A. Ochrymowycz and D. B. Rorabacher, *Inorg. Chem.*, 1995, **34**, 6053–6064.
5 B. C. Dunn, L. A. Ochrymowycz and D. B. Rorabacher, *Inorg. Chem.*, 1997, **36**, 3253–3257.
6 P. Wijetunge, C. P. Kulatilleke, L. T. Dressel, M. J. Heeg, L. A. Ochrymowycz and D. B. Rorabacher, *Inorg. Chem.*, 2000, **39**, 2897–2905.
7 Q. Yu, C. A. Salhi, E. A. Ambundo, M. J. Heeg, C. P. Kulatilleke, L. A. Ochrymowycz and D. B. Rorabacher, *J. Am. Chem. Soc.*, 2001, **124**, 5720–5729.
8 N. Koshino, Y. Kuchiyama, S. Funahashi and H. D. Takagi, *Can. J. Chem.*, 1999, **77**, 1498–1507.
9 N. Koshino, Y. Kuchiyama, H. Ozaki, S. Funahashi and H. D. Takagi, *Inorg. Chem.*, 1999, **38**, 3352–3360.
10 N. Koshino, Y. Kuchiyama, S. Funahashi and H. D. Takagi, *Chem. Phys. Lett.*, 1999, **306**, 291–296.
11 N. Koshino, S. Itoh, Y. Kuchiyama, S. Funahashi and H. D. Takagi, *Inorg. React. Mech.*, 2000, **2**, 93–99.
12 S. Itoh, S. Funahashi, N. Koshino and H. D. Takagi, *Inorg. Chim. Acta*, 2001, **324**, 252–265.
13 N. M. Villeneuve, R. R. Schroeder, L. A. Ochrymowycz and D. B. Rorabacher, *Inorg. Chem.*, 1997, **36**, 4475–4483.
14 B. Bosnich, C. K. Poon and M. L. Tobe, *Inorg. Chem.*, 1965, **4**, 1102–1108.
15 P. A. Tasker and L. Sklar, *J. Cryst. Mol. Struct.*, 1975, 329–344.
16 J. Elmsley, M. Arif, P. A. Bates and M. B. Hursthouse, *J. Mol. Struct.*, 1990, **220**, 1–12.
17 X. Chen, G. Long, R. D. Willett, T. Hawks, S. Molnar and K. Brewer, *Acta Crystallogr., Sect. C*, 1996, **52**, 1924–1928.
18 H. Oshio, *Inorg. Chem.*, 1993, **32**, 4123–4130.
19 H. Ohtaki and H. Seki, *J. Macromol. Sci., Chem.*, 1990, **A27**, 1305–1319.
20 S. Matsuo, T. Yamaguchi and H. Wakita, *Adv. Quantum Chem.*, 2001, **37**, 153–162.
21 D. T. Pierce, T. L. Hatfield, E. J. Billo and Y. Ping, *Inorg. Chem.*, 1997, **36**, 2950–2955.
22 M. D. Glick, D. P. Gavel, L. L. Diaddario and D. B. Rorabacher, *Inorg. Chem.*, 1976, **15**, 1190–1193.
23 M. M. Bernardo, M. J. Heeg, R. R. Schroeder, L. A. Ochrymowycz and D. B. Rorabacher, *Inorg. Chem.*, 1992, **31**, 191–198.
24 M. A. Donnelly and M. Zimmer, *Inorg. Chem.*, 1999, **38**, 1650–1658.
25 R. Clay, J. Murray-Rust and P. Murray-Rust, *J. Chem. Soc., Dalton Trans.*, 1979, 1135–1139.
26 J. C. A. Boeyens, *Acta Crystallogr., Sect. C*, 1983, **39**, 846–849.
27 Isocyclam ([14]aneN$_4$-*b*) also readily forms folded (*cis*) complexes with Ni(II): Y. Satake, Y. Ihara, H. Senda, M. Suzuki and A. Uehara, *Inorg. Chem.*, 1992, **31**, 3248–3251.
28 T. H. Tahirov, Y.-H. Lu, W.-J. Lan and C.-S. Chung, *Acta Crystallogr., Sect. C*, 1993, **49**, 1908–1910.
29 A. Schiegg, A. Riesen and T. A. Kaden, *Helv. Chim. Acta*, 1991, **74**, 1689–1696.
30 T.-H. Lu, K. Panneerselvam, S.-F. Tung, T.-Y. Chi and C.-S. Chung, *Acta Crystallogr., Sect. C*, 1997, **53**, 1780–1782.
31 R. C. Luckay and R. D. Hancock, *J. Chem. Soc., Dalton Trans.*, 1991, 1491–1494.
32 P. Zanello, R. Seeber, A. Cinquantini, G.-A. Mazzocchin and L. Fabbrizzi, *J. Chem. Soc., Dalton Trans.*, 1982, 893–897.
33 We have avoided using the term "iso-[14]aneS$_4$" for this ligand since that term has previously been applied as a designation for 1,4,7,10-tetrathiacyclotetradecane (chelate ring sequence 5,5,5,7): V. V. Pavlishchuk, K. B. Yatsimirskii, P. E. Strizhak and J. Labuda, *Inorg. Chim. Acta*, 1989, **164**, 65–68.
34 L. S. W. Sokol, L. A. Ochrymowycz and D. B. Rorabacher, *Inorg. Chem.*, 1981, **20**, 3189–3195.
35 L. L. Diaddario, L. L. Zimmer, T. E. Jones, L. S. W. L. Sokol, R. B. Cruz, E. L. Yee, L. A. Ochrymowycz and D. B. Rorabacher, *J. Am. Chem. Soc.*, 1979, **101**, 3511–3520.
36 M. M. Bernardo, R. R. Schroeder and D. B. Rorabacher, *Inorg. Chem.*, 1991, **30**, 1241–1247.
37 B. C. Westerby, K. L. Juntunen, G. H. Leggett, V. B. Pett, M. J. Koenigbauer, M. D. Purgett, M. J. Taschner, L. A. Ochrymowycz and D. B. Rorabacher, *Inorg. Chem.*, 1991, **30**, 2109–2120.

38 L. Aronne, B. C. Dunn, J. R. Vyvyan, C. W. Souvignier, M. J. Mayer, T. A. Howard, C. A. Salhi, S. N. Goldie, L. A. Ochrymowycz and D. B. Rorabacher, *Inorg. Chem.*, 1995, **34**, 357–369.
39 L. A. Ochrymowycz, C.-P. Mak and J. D. Michna, *J. Org. Chem.*, 1974, **39**, 2079–2084.
40 N. Li, C. M. Eberlein, W. A. Volkert, L. Ochrymowycz, C. Barnes and A. R. Ketring, *Radiochim. Acta*, 1996, **75**, 83–95.
41 J. Houk and G. M. Whitesides, *J. Am. Chem. Soc.*, 1987, **109**, 6825–6836.
42 L. L. Diaddario, Jr., L. A. Ochrymowycz and D. B. Rorabacher, *Inorg. Chem.*, 1992, **31**, 2347–2353.
43 G. Sheldrick, SHELX-86, SHELXL-93 and SADABS, University of Göttingen, Germany, 1986, 1993 and 1996.
44 E. L. Yee, R. J. Cave, K. L. Guyer, P. D. Tyma and M. J. Weaver, *J. Am. Chem. Soc.*, 1979, **101**, 1131–1137.
45 Q. Yu, A. Kandegedara, Y. Xu and D. B. Rorabacher, *Anal. Biochem.*, 1997, **253**, 50–56.
46 A. Kandegedara and D. B. Rorabacher, *Anal. Chem.*, 1999, **71**, 3140–3144.
47 A. E. Martell, R. J. Motekaitis, *Determination and Use of Stability Constants*, VCH Publishers: New York, 2nd edn.,1992.
48 H. McConnell and N. Davidson, *J. Am. Chem. Soc.*, 1950, **72**, 3164-3167 Cf., H. Benesi and J. H. Hildebrand, *J. Am. Chem. Soc.*, 1949, **71**, 2703–2707.
49 B. C. Dunn, P. Wijetunge, J. R. Vyvyan, T. A. Howard, A. J. Grall, L. A. Ochrymowycz and D. B. Rorabacher, *Inorg. Chem.*, 1997, **36**, 4484–4489.
50 Ref. 23, footnote 39.
51 E. A. Ambundo, M.-V. Deydier, L. A. Ochrymowycz and D. B. Rorabacher, *Inorg. Chem.*, 2000, **39**, 1171–1179.
52 By contrast, the structure of the tetrafluoroborate salt of the Pd(II) complex with a related 5,5,6,6 ligand, 1,4,7-trithia-11-azacyclotetradecane, shows that the ligand is in conformer I: B. Chak, A. McAuley and T. W. Whitcombe, *Inorg. Chim. Acta*, 1996, **246**, 349–360; however, this conformer is presumably influenced by the larger size of the Pd(II) ion as suggested by the similarity of this structure to that for $[Cu^{II}([13]aneS_4)(H_2O)](ClO_4)_2$: V. B. Pett, L. L. Diaddario, Jr., E. R. Dockal, P. W. R. Corfield, C. Ceccarelli, M. D. Glick, L. A. Ochrymowycz and D. B. Rorabacher, *Inorg. Chem.*, 1983, **22**, 3661–3670.
53 E. R. Dockal, L. L. Diaddario, M. D. Glick and D. B. Rorabacher, *J. Am. Chem. Soc.*, 1977, **99**, 4530–4532.
54 P. W. R. Corfield, C. Ceccarelli, M. D. Glick, I. W.-Y. Moy, L. A. Ochrymowycz and D. B. Rorabacher, *J. Am. Chem. Soc.*, 1985, **107**, 2399–2404.
55 The formation rate constant for Cu(II) reacting with diprotonated [14]aneN_4-*b* is reported to be nearly 400 times larger than for the corresponding value with [14]aneN_4-*a*. However, this probably reflects a difference in internal hydrogen bonding for the two H_2L^{2+} species since similar formation rate constants were obtained for the two monoprotonated ligands with Co(II), Ni(II) and Zn(II): P. Grunow-Schultz and T. A. Kaden, *Helv. Chim. Acta*, 1978, **61**, 2291–2296.
56 C. P. Kulatilleke, S. N. Goldie, M. J. Heeg, L. A. Ochrymowycz and D. B. Rorabacher, *Inorg. Chem.*, 2000, **39**, 1444–1453.
57 B.-F. Liang and C.-S. Chung, *Inorg. Chem.*, 1980, **19**, 1867–1871.
58 B.-F. Liang and C.-S. Chung, *Inorg. Chem.*, 1981, **20**, 2152–2155.
59 R. A. Marcus and N. Sutin, *Biochim. Biophys. Acta*, 1985, **811**, 265–322.
60 G. H. Leggett, B. C. Dunn, A. M. Q. Vande Linde, L. A. Ochrymowycz and D. B. Rorabacher, *Inorg. Chem.*, 1993, **32**, 5911–5918.
61 B. M. Hoffman and M. A. Ratner, *J. Am. Chem. Soc.*, 1987, **109**, 6237–6243; *cf.*, B. M. Hoffman and M. A. Ratner, *J. Am. Chem. Soc.*, 1988, **110**, 8267.
62 B. S. Brunschwig and N. Sutin, *J. Am. Chem. Soc.*, 1989, **111**, 7454–7465.